



# Nanoporous Single-Crystal-Like $\text{Cd}_x\text{Zn}_{1-x}\text{S}$ Nanosheets Fabricated by the Cation-Exchange Reaction of Inorganic–Organic Hybrid ZnS–Amine with Cadmium Ions\*\*

Yifu Yu, Jin Zhang, Xuan Wu, Weiwei Zhao, and Bin Zhang\*

Dedicated to Professor Yiling Tian on the occasion of his 65th birthday

Porous nanostructures have received considerable attention because of their improved chemical and physical performance over solid materials<sup>[1–2]</sup> as well as their intriguing applications<sup>[3]</sup> in nanoreactors, actuators, energy storage, solar cells, ultrafiltration and separation,  $\text{CO}_2$  capture, catalysis, cell imaging, and drug delivery. Among materials with various shapes, nanosheets have attracted intensive interests as sheetlike materials with predominantly exposed crystal facets may exhibit improved catalytic performance over their wirelike or spherical structures.<sup>[4]</sup> But, the efficient synthesis of porous single-crystalline sheets still remains a challenge. Thus, their improved properties and promising applications are driving researchers to develop facile strategies to synthesize porous sheetlike materials, especially with adjustable composition and pore size.

Since the discovery by Alivisato and co-workers of the cation-exchange reaction in nanocrystals,<sup>[5]</sup> much attention has been paid to the transformation of one crystalline material to another through cation exchange in aqueous solution.<sup>[6]</sup> At present, research efforts mainly focus on the modulation of the composition, structure, and properties of solid inorganic nanocrystals and nanowires.<sup>[6]</sup> In these cases, some hollow regions are produced because of the Kirkendall effect.<sup>[6]</sup> Recently, metal–organic frameworks and coordinating compounds have been found to exhibit unique cation-exchange properties.<sup>[7]</sup> Our previous study demonstrated that vapor-phase cation-exchange reactions of CdS with organic zinc could generate 1D nanostructures with adjustable composition and morphology.<sup>[8]</sup> Although these advances have been achieved, the development of solution-phase cation-exchange reactions for the synthesis of nanoporous 1D and 2D nanostructures, especially sheetlike materials with predominantly exposed crystal facets, is still in its infancy.

The inorganic–organic hybrid nanomaterials can be used as a template for the preparation of functional materials.<sup>[9]</sup> For example, Yu and co-workers found that hybrid nanowires could be transformed into inorganic nanotubes by removing the organic components in selected solvents.<sup>[9b]</sup> The thermal decomposition of hybrid materials in air can lead to the formation of porous oxides.<sup>[9c]</sup> However, to the best of our knowledge, there are few reports on using hybrid semiconductors as starting materials for ion-exchange reactions to produce porous materials with modulated pore size and composition.

Here we adopt the inorganic–organic hybrid semiconductor sheets as the starting materials and describe a facile cation-exchange strategy to fabricate single-crystal-like porous nanosheets. We show that nanoporous inorganic  $\text{Cd}_x\text{Zn}_{1-x}\text{S}$  nanosheets with controlled pore size and adjustable composition are accessible by this approach. The as-prepared single-crystal-like porous  $\text{Cd}_{0.5}\text{Zn}_{0.5}\text{S}$  nanosheets are highly active for photocatalytic  $\text{H}_2$  evolution from water splitting. In addition, the cation-exchange strategy of inorganic–organic hybrid materials is suitable for fabricating other porous nanostructures.

To demonstrate the cation-exchange method of hybrid materials for producing porous nanostructures, transforming inorganic–organic hybrid ZnS–diethylenetriamine (DETA) into porous  $\text{Cd}_x\text{Zn}_{1-x}\text{S}$  nanosheets is selected as the model system. As shown in Figure 1a, the ZnS–DETA nanosheets are first prepared using a modified amine-assisted hydrothermal method, and then react with different concentrations of  $\text{Cd}^{2+}$  cations to obtain nanoporous  $\text{Cd}_x\text{Zn}_{1-x}\text{S}$  and CdS (see the Supporting Information). The ZnS–DETA nanosheets are firstly examined using scanning electron microscopy (SEM). The SEM images (the inset in Figure 1b and Figure S1-1a in the Supporting Information) clearly show that ZnS–DETA nanosheets were successfully fabricated in high yields. Typical X-ray diffraction (XRD) pattern of the as-prepared hybrid precursors identify them as the ZnS–(DETA)<sub>0.5</sub> (see Figure S1e in the Supporting Information). When the ZnS–DETA nanosheets exchange with  $\text{Cd}^{2+}$  cations, solid sheets become nanoporous (see Figure 1e). After the hybrid precursors have reacted with excessive  $\text{Cd}^{2+}$  cations, the completely exchanged products are nanoporous CdS nanosheets with a pore size of 10–50 nm (see Figure 1g,h and Figure S1-1c,d in the Supporting Information) and a thickness of around 20 nm (see Figure S1-2 in the Supporting Information). FTIR spectra shown in Figure S1-1f in the

[\*] Dr. Y. Yu,<sup>[†]</sup> J. Zhang,<sup>[†]</sup> X. Wu, W. Zhao, Prof. Dr. B. Zhang  
Department of Chemistry, School of Science  
Tianjin University, Tianjin 300072 (P.R. China)  
E-mail: bzhang@tju.edu.cn

[†] Both authors contributed equally to this work.

[\*\*] This work was financially supported by the National Natural Science Foundation of China (No. 20901057, 11074185, and 20806059), the Tianjin Natural Science Foundation (No. 10JCYBJC01800), the State Key Laboratory of Crystal Material at Shandong University (No. KF0910) and the Innovation Foundation of Tianjin University.

Supporting information for this article is available on the WWW under <http://dx.doi.org/10.1002/ange.201105786>.

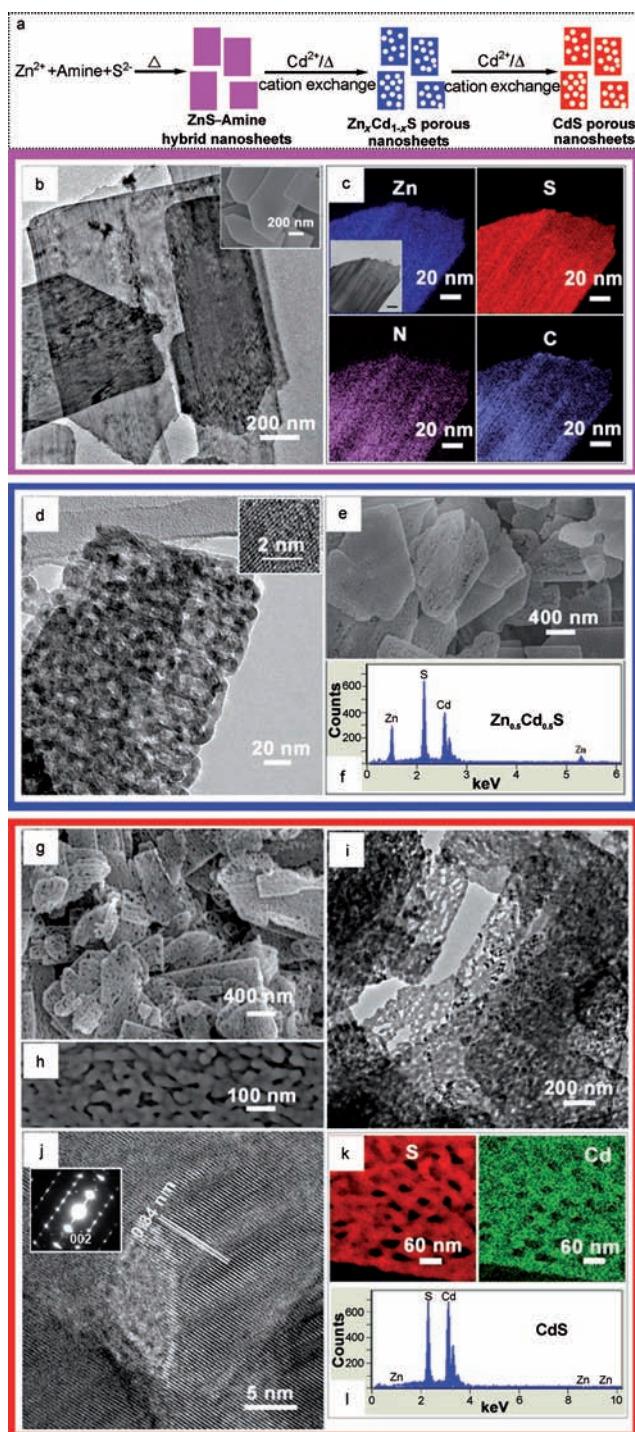


**Figure 1.** a) Nanoporous sheets with adjustable composition prepared through the cation-exchange strategy of the inorganic–organic hybrid sheets. b–c) TEM and SEM images (b and the inset), and EELS elemental mapping images (c) of the ZnS–DETA hybrid sheets. d–f) TEM and HRTEM images (d and its inset), SEM image, and EDX spectrum of the nanoporous  $\text{Cd}_{0.5}\text{Zn}_{0.5}\text{S}$  nanosheets. g–l) SEM (g, h), TEM (i), HRTEM images and the associated SEAD pattern (j and its inset), EELS elemental mapping images (k), and EDX spectrum (l) of single-crystal-like nanoporous CdS nanosheets obtained by the cation-exchange strategy of hybrid precursors.

Supporting Information also confirm that the hybrid precursors can be successfully transformed into inorganic materials.

These nanoporous sheets are assigned to the hexagonal phase of CdS by the XRD patterns (see Figure S1–1e in the Supporting Information). These results imply cation-exchange reactions of the inorganic–organic hybrid materials with cadmium cations can lead to the formation of nanoporous inorganic nanosheets.

The structure transformations induced by cation exchange are further characterized using transmission electron microscopy (TEM) and electron energy loss spectroscopy (EELS). Figure 1b,c shows TEM images and EELS elemental mapping images of ZnS–DETA hybrid nanosheets, respectively, suggesting that the flake-like hybrid precursors contain N, S, C, Zn elements. When the molar ratio of ZnS–DETA to  $\text{Cd}^{2+}$  is 2:1, the nanoporous sheets with a pore size of around 20 nm are obtained (see Figure 1d,e). Clearly observed lattice fringes in a HRTEM image (the inset in Figure 1d) indicate the single-crystal-like structure of nanoporous sulfide nanosheets. The point-scan energy dispersive X-ray spectrum (see Figure 1f) shows that porous nanosheets of the composition  $\text{Cd}_{0.5}\text{Zn}_{0.5}\text{S}$ , which is in accordance with the molar ratio of agents added. When enough  $\text{Cd}^{2+}$  cations are adopted to react with ZnS–DETA nanosheets, nanoporous CdS sheets, the completely exchanged products, can be generated, as confirmed by TEM and EDX spectra (see Figure 1i,l). EELS elemental mapping images (see Figure 1k) imply that the nanoporous sheets are composed of Cd and S. The HRTEM image and the associated selected electron diffraction (SAED; see Figure 1j) pattern show that the as-prepared nanoporous CdS sheets are single-crystalline. These results show that the single-crystal-like  $\text{Cd}_x\text{Zn}_{1-x}\text{S}$  with adjustable composition can be successfully obtained by changing the relative ratio of hybrid precursors to cation in the current approach.

The pore size of the nanoporous sheet of  $\text{Cd}_x\text{Zn}_{1-x}\text{S}$  can be modulated by varying the solvent. When water is used as the solvent for cation-exchange reactions and the molar ratio of ZnS–DETA to  $\text{Cd}^{2+}$  is 1:2, the products are nanoporous CdS nanosheets with pore sizes of about 10–50 nm (see Figure S2 in the Supporting Information). The pore size of porous CdS nanosheets experiences an obvious decrease to around 10–20 nm (see Figure S3 in the Supporting Information) when the exchange reaction is performed in ethylene glycol whereas other conditions remain unchanged. The solvent has a noticeable influence on the pore size of the ion-exchanged products, which may be associated with the solvability of DETA in different solvents. Size distributions of two different porous CdS nanosheets (see Figure S4 in the Supporting Information) confirm that the pore size modulation can be accomplished by changing the reacting solvents, which may be important for investigating size effects of the pores on the chemical and physical properties. Representative nitrogen adsorption/desorption isotherms (see Figure S4 in the Supporting Information) display the typical character of IV-type isothermal curves, suggesting that the mesoporous structure of the nanoporous nanosheets is obtained.

Furthermore, this strategy presented here can be broadened to the synthesis of nanoporous metal selenides and oxides with single-crystal-like structures. For instance, when ZnSe–DETA nanosheets are used as starting materials for



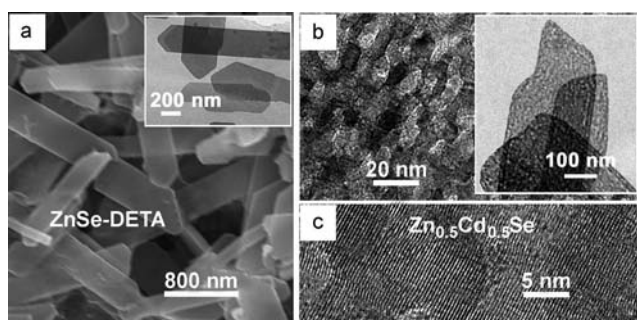


**Figure 2.** a) SEM and TEM (the inset) images of the ZnSe-DETA hybrid sheets. b–c) TEM (b and its inset) and HRTEM (c) images of nanoporous single-crystal-like  $\text{Cd}_{0.5}\text{Zn}_{0.5}\text{S}$  nanosheets, indicating the generality of the cation-exchange protocol of hybrid precursors in generating nanoporous single-crystal-like sheets.

cation-exchange reactions with  $\text{Cd}^{2+}$  cations, porous  $\text{Cd}_x\text{Zn}_{1-x}\text{S}$  single-crystal-like nanosheets can also be generated, (see Figure 2 and Figure S5 in the Supporting Information). In addition, the as-prepared  $\text{CeO}_2$ -amine nanowires can be transformed into nanoporous  $\text{Ce}_x\text{Zr}_{1-x}\text{O}_2$  single-crystal-like nanowires through cation exchange with  $\text{ZrOCl}_2$  in aqueous media (see Figure S6 in the Supporting Information). These extending works indicate that our cation-exchange protocol of inorganic–organic hybrid composites is successful for producing porous nanostructures and may be developed into a generalized strategy for preparing porous single-crystalline nanostructures.

To understand the growth mechanism of nanoporous sheet-like nanostructures prepared by the cation-exchange reaction method, TEM, HRTEM, and EDX were used to characterize the intermediates collected at different reaction stages. When the cation-exchange reaction proceeds for 0.5 h, the sheets become rough with voids (see Figure S7a,b in the Supporting Information). The associated EDX spectrum (see Figure S7c in the Supporting Information) reveals that most of the zinc ions in ZnS-DETA have been exchanged with cadmium cations in a very short time, suggesting the rapid kinetics of this cation-exchange reactions. But, we find that the exchange of cadmium in Cd-DETA with zinc cations cannot occur under the same condition. This may suggest that the driving force for the cation exchange is the enthalpy-driven formation of CdS which makes the reaction thermodynamically favorable.<sup>[8,10]</sup> The appearance of voids can be attributed to the rapid kinetic and stain release because of the large lattice mismatch (7–8%). Similar strain-driven formation of hollow structures has been observed and theoretically predicted for partial cation exchange<sup>[11]</sup> and sulfidation/oxidation of nanocrystals.<sup>[12]</sup> In addition, the dissolution of DETA in aqueous solution is responsible for the appearance of voids. In fact, when the inorganic–organic ZnS-DETA nanosheets were treated in aqueous solution in the absence of  $\text{Cd}^{2+}$  cations and the other conditions remain unchanged, the hybrid nanosheets transformed into ZnS nanoparticles (see Figure S8 in the Supporting Information), suggesting that DETA in the hybrid sheets can be dissolved in water. With the continuous increase of the reaction time, the ratio of zinc in  $\text{Cd}_x\text{Zn}_{1-x}\text{S}$ -amine is decreasing, and the pores become

bigger because of the correlating roles of the strain-driven voids and the dissolution of DETA in aqueous media during cation-exchange reactions. This finally leads to the formation of nanoporous CdS nanosheets with single-crystal-like structure (see Figure 1 g–i).

Recently, metal sulfide nanostructures have been found to show significant catalytic activity for the photocatalytic hydrogen generation from water splitting (PHWS).<sup>[13]</sup> Here, PHWS is tested for comparative studies on the catalytic activity of porous single-crystal-like  $\text{Zn}_{0.5}\text{Cd}_{0.5}\text{S}$  nanosheets (C-I) and  $\text{Zn}_{0.5}\text{Cd}_{0.5}\text{S}$  nanorods (C-II). UV/Vis diffuse reflectance spectra (DRS; see Figure 3 a) show that the spectrum of C-I

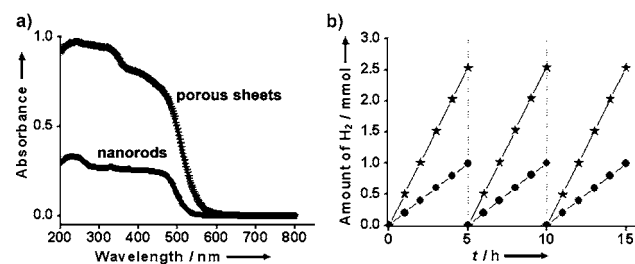


**Figure 3.** a) UV/Vis diffuse reflectance spectra and b) time course of evolved  $\text{H}_2$  under irradiation of visible light of the as-prepared  $\text{Zn}_{0.5}\text{Cd}_{0.5}\text{S}$  porous nanosheets (\*) and  $\text{Zn}_{0.5}\text{Cd}_{0.5}\text{S}$  nanorods (●).

shifts to longer wavelengths relative to the spectrum of C-II, corresponding to a decrease in the band gap.<sup>[14]</sup> In addition, the absorption region of C-I is much steeper and higher than that of C-II, indicating the stronger absorption ability of C-I relative to that of C-II. Figure 3 b displays the reaction time courses for  $\text{H}_2$  evolution over C-I and C-II. As displayed in Figure 3 b, the photocatalytic reaction upon C-I shows a stable  $\text{H}_2$  release rate of around  $0.5 \text{ mmol h}^{-1}/0.3 \text{ g}$ , which is about 2.5 times that of C-II. The improved activity of C-I may be associated with its narrower band gap<sup>[13c,14]</sup> and stronger absorption ability of photons. The single-crystal-like structure reduced the number of defects, where the photogenerated electrons and holes recombine.<sup>[13c]</sup> In comparison with other solid nanostructures, porous structures not only possess larger active surface area and much more active sites,<sup>[13c–e]</sup> but they also effectively prevent the agglomeration of catalysts. In addition, networklike porous nanosheets might also shorten the distance between the generation center and the active surface, and make it possible for electrons to migrate easily to surface active sites. The cation-exchange strategy of hybrid materials presented here may be a step forward to the synthesis of novel porous single-crystal-like nanomaterials for  $\text{H}_2$  production.

In summary, we report the synthesis of nanoporous single-crystal-like  $\text{Cd}_x\text{Zn}_{1-x}\text{S}$  nanosheets with good structural stability by cation-exchange reactions of the prepared ZnS-DETA hybrid nanosheets with  $\text{Cd}^{2+}$  cations. The pore size and composition of the nanoporous  $\text{Cd}_x\text{Zn}_{1-x}\text{S}$  sheets are modulated by changing the solvent and cadmium ions, respectively. The formation of nanopores is possibly associated with the dissolution of organic components of the hybrid nanosheets during

the cation-exchange reaction. The porous  $\text{Cd}_x\text{Zn}_{1-x}\text{S}$  nanosheets show a higher catalytic performance relative to their solid crystals for the photocatalytic  $\text{H}_2$  evolution from water splitting. The improvement may be attributed to the narrow band gap and strong absorption ability of photons, the intrinsic single-crystal-like properties, and the unique configuration of porous  $\text{Cd}_x\text{Zn}_{1-x}\text{S}$  nanosheets. We also show that this cation-exchange strategy of hybrid nanostructures can be extended to the preparation of nanoporous metal selenides and oxides. The present work may open a new general route for the fabrication of single-crystal-like porous inorganic nanomaterials with enhanced chemical/physical performance.

Received: August 16, 2011

Published online: October 11, 2011

**Keywords:** cation exchange · mesoporous materials · nanostructures · photocatalysis

- [1] a) A. Wittstock, V. Zielasek, J. Biener, C. M. Friend, M. Bäumer, *Science* **2010**, 327, 319–322; b) C. Xu, L. Wang, R. Wang, K. Wang, Y. Zhang, F. Tian, Y. Ding, *Adv. Mater.* **2009**, 21, 2165–2169; c) A. Chen, P. Holt-Hindle, *Chem. Rev.* **2010**, 110, 3767–3804; d) B. C. Tappan, S. A. Steiner III, E. P. Luther, *Angew. Chem.* **2010**, 122, 4648–4669; *Angew. Chem. Int. Ed.* **2010**, 49, 4544–4565; e) Z. Peng, H. Yang, *J. Am. Chem. Soc.* **2010**, 131, 7542–7543; f) S. Wang, Z. Liu, D. Wang, C. Li, C. Chen, Y. Yin, *J. Mater. Chem.* **2011**, 21, 6365–6369.
- [2] a) J. Ye, W. Liu, J. Cai, S. Chen, X. Zhao, H. Zhou, L. Qi, *J. Am. Chem. Soc.* **2011**, 133, 933–940; b) S. M. Paek, E. J. Yoo, I. Honma, *Nano Lett.* **2009**, 9, 72–75; c) D. Borisova, H. Mohwald, D. G. Shchukin, *ACS Nano* **2011**, 5, 1939–1946; d) C. K. Tsung, J. Fan, N. Zheng, Q. Shi, A. J. Forman, J. Wang, G. D. Stucky, *Angew. Chem.* **2008**, 120, 8810–8814; *Angew. Chem. Int. Ed.* **2008**, 47, 8682–8686; e) F. Sauvage, D. H. Chen, P. Comte, F. Z. Huang, L. P. Heiniger, Y. B. Cheng, R. A. Caruso, M. Graetzel, *ACS Nano* **2010**, 4, 4420–4425; f) J. Brillet, M. Grätzel, K. Sivula, *Nano Lett.* **2010**, 10, 4155–4160; g) L. Jia, W. Cai, H. Wang, F. Sun, Y. Li, *ACS Nano* **2009**, 9, 2697–2705.
- [3] a) J. Liu, S. Z. Qiao, S. B. Hartono, G. Q. Lu, *Angew. Chem.* **2010**, 122, 5101–5105; *Angew. Chem. Int. Ed.* **2010**, 49, 4981–4985; b) Y. Liang, M. G. Schwab, L. Zhi, E. Mugnaioli, U. Kolb, X. Feng, K. Müllen, *J. Am. Chem. Soc.* **2010**, 132, 15030–15037; c) Y. Chen, H. R. Chen, D. P. Zeng, Y. B. Tian, F. Chen, J. W. Feng, J. L. Shi, *ACS Nano* **2010**, 4, 6001–6013; d) H. J. Jin, X. L. Wang, S. Parida, K. Wang, M. Seo, J. Weissmüller, *Nano Lett.* **2010**, 10, 187–194; e) J. Biener, A. Wittstock, L. A. Zepdear, Ruiz, M. M. Biener, V. Zielasek, D. Kramer, R. N. Viswanath, J. Weissmüller, M. Bäumer, A. V. Hamza, *Nat. Mater.* **2009**, 8, 47–51; f) S. C. Xiang, Z. J. Zhang, C. G. Zhao, K. L. Hong, X. B. Zhao, D. R. Ding, M. H. Xie, C. D. Wu, M. C. Das, R. Grill, K. M. Thomas, B. L. Chen, *Nat. Commun.* **2011**, 2, 204.
- [4] a) H. G. Yang, C. H. Sun, S. Z. Qiao, J. Zou, G. Liu, S. C. Smith, H. M. Cheng, G. Q. Lu, *Nature* **2008**, 453, 638–641; b) H. G. Yang, G. Liu, S. Z. Qiao, C. H. Sun, Y. G. Jin, S. C. Smith, J. Zou, H. M. Cheng, G. Q. Lu, *J. Am. Chem. Soc.* **2009**, 131, 4078–4083; c) X. Xie, Y. Li, Z. Q. Liu, M. Haruta, W. Shen, *Nature* **2009**, 458, 746–747; d) C. Z. Wen, H. B. Jiang, S. Z. Qiao, H. G. Yang, G. Q. Lu, *J. Mater. Chem.* **2011**, 21, 7052–7061.
- [5] D. H. Son, S. M. Hughes, Y. D. Yin, A. P. Alivisatos, *Science* **2004**, 306, 1009–1012.
- [6] a) R. D. Robinson, B. Sadtler, D. O. Demchenko, C. K. Erdonmez, L. W. Wang, A. P. Alivisatos, *Science* **2007**, 317, 355–358; b) X. Liang, X. Wang, Y. Zhuang, B. Xu, S. Kuang, Y. Li, *J. Am. Chem. Soc.* **2007**, 129, 2736–2737.
- [7] a) A. Deák, T. Tunyogi, G. Palinkas, *J. Am. Chem. Soc.* **2009**, 131, 2815–2817; b) S. L. Huang, X. X. Li, X. J. Shi, H. W. Hou, Y. T. Fan, *J. Mater. Chem.* **2010**, 20, 5695–5699.
- [8] B. Zhang, Y. Jung, H. S. Chung, L. Van Vugt, R. Agarwal, *Nano Lett.* **2010**, 10, 149–155.
- [9] a) M. R. Gao, W. T. Yao, H. B. Yao, S. H. Yu, *J. Am. Chem. Soc.* **2009**, 131, 7486–7487; b) M. Zhang, Y. Lu, J. F. Chen, T. K. Zhang, Y. Y. Liu, Y. Yang, W. T. Yao, S. H. Yu, *Langmuir* **2010**, 26, 12882–12889; c) Z. A. Zang, H. B. Yao, Y. X. Zhou, W. T. Yao, S. H. Yu, *Chem. Mater.* **2008**, 20, 4749–4755.
- [10] S. E. Wark, D. S. Kim, J. Park, *Chem. Mater.* **2007**, 19, 4663–4669.
- [11] S. E. Wark, C. H. Hsia, D. H. Son, *J. Am. Chem. Soc.* **2008**, 130, 9550–9555.
- [12] a) A. Cabot, R. K. Smith, Y. D. Yin, H. M. Zheng, B. M. Reinhard, H. T. Liu, A. P. Alivisatos, *ACS Nano* **2008**, 2, 1452–1458; b) V. P. Zhdanov, B. Kasemo, *Nano Lett.* **2009**, 9, 2172–2176; c) Y. F. Yu, S. X. Hou, M. Meng, X. T. Tao, W. X. Liu, Y. L. Lai, B. Zhang, *J. Mater. Chem.* **2011**, 21, 10525–10531.
- [13] a) F. E. Osterloh, *Chem. Mater.* **2008**, 20, 35–54; b) X. Zong, H. J. Yan, G. P. Wu, G. J. Ma, F. Y. Wen, L. Wang, C. Li, *J. Am. Chem. Soc.* **2008**, 130, 7176–7177; c) A. Kudo, Y. Miseki, *Chem. Soc. Rev.* **2009**, 38, 253–278; d) N. Z. Bao, L. M. Shen, T. Takata, K. Domen, *Chem. Mater.* **2008**, 20, 110–117; e) N. Zheng, X. H. Bu, H. Vu, P. Y. Feng, *Angew. Chem.* **2005**, 117, 5433–5437; P. Y. Feng, *Angew. Chem.* **2005**, 117, 5433–5437; *Angew. Chem. Int. Ed.* **2005**, 44, 5299–5303; f) I. Tsuji, H. Kato, A. Kudo, *Angew. Chem.* **2005**, 117, 3631–3634; *Angew. Chem. Int. Ed.* **2005**, 44, 3565–3568.
- [14] F. Zuo, L. Wang, T. Wu, Z. Y. Zhang, D. Borchardt, P. Y. Feng, *J. Am. Chem. Soc.* **2010**, 132, 11856–11857.